analytical chemistry

Article

pubs.acs.org/ac

Comprehensive Dual Liquid Chromatography with Quadruple Mass Spectrometry (LC1MS2 × LC1MS2 = LC2MS4) for Analysis of *Parinari Curatellifolia* and Other Seed Oil Triacylglycerols

William C. Byrdwell*

Food Composition and Methods Development Lab, Agricultural Research Service, Beltsville Human Nutrition Research Center, USDA, 10300 Baltimore Avenue, Building 161, Beltsville, Maryland 20705, United States

Supporting Information

ABSTRACT: Online two-dimensional (2D) comprehensive liquid chromatography (LC × LC) has become increasingly popular. Most LC × LC separations employ one or more detectors at the outlet of the second dimension, ^{2}D, with very short runs to avoid undersampling. We used six detectors, including dual parallel mass spectrometry (LC1MS2), for detection of the first dimension, ^{1}D. We made an argentation (silver-ion) UHPLC column from a strong cation exchange column for ^{2}D, coupled with UV and LC1MS2 detection. LC1MS2 in ^{1}D combined with LC1MS2 in ^{2}D, plus five other detectors, constituted LC2MS4 in a comprehensive LC1MS2 × LC1MS2 2D-LC separation. Electrospray ionization (ESI) high resolution accurate mass (HRAM) mass spectrometry (MS) and atmospheric pressure chemical ionization (APCI) MS were used in parallel for ^{1}D detection, while atmospheric pressure photoionization (APPI) MS and ESI-MS were used for detection of ^{2}D. The LC1MS2 used for ^{1}D allowed quantification of triacylglycerol (TAG) molecular species of *Parinari curatellifolia* and other seed oils, while the ^{2}D allowed isomers of TAG containing 18:3 fatty acyl chains as well as TAG regioisomers to be separated and identified. The LC1MS2 in ^{1}D allowed identification of oxo-TAG species by HRAM MS and quantification of 806.3 ± 1.3 and 1101 ± 22 μg/g of α- and γ-tocopherols, respectively, in *P. curatellifolia* by APCI-MS. It is now feasible to use silver-ion UHPLC as the ^{2}D separation in LC × LC and to use multiple mass spectrometers across both dimensions to perform conventional quantitative analysis and to take advantage of the newest LC × LC separation technology to identify isomers that are otherwise difficult to separate.

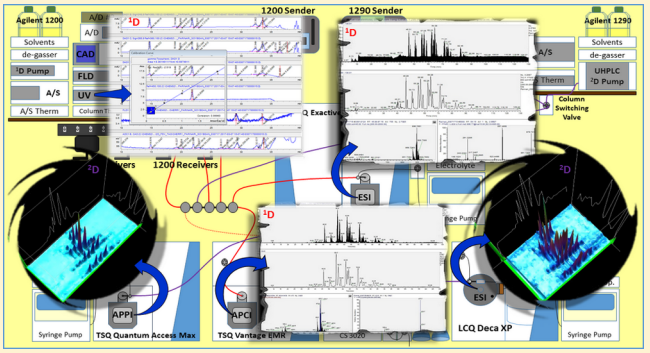

Numerous reviews of two-dimensional liquid chromatography (2D-LC) techniques have appeared in recent years, with those covering basic theory and principles[1−3] and describing 2D-LC coupled to mass spectrometry[4] (MS) being especially useful for the work described herein. Excellent chapters describing both theoretical and practical aspects with citations for numerous reviews and applications in a wide range of fields have recently appeared.[5,6] Note that the nomenclature of Marriott et al.[7] and Schoenmakers et al.,[8] as reflected in the chapter by Stoll,[6] is used here. Although the peak capacity in LC × LC is theoretically multiplicative (the product of the 1D-LC peak capacities) if the 2D separations are perfectly orthogonal, but in practice the maximum theoretical peak capacity is rarely achieved.[6] Nevertheless, it is typically possible to achieve a higher (often much higher) peak capacity by employing 2D-LC rather than 1D-LC.

Conventional LC × LC is typically done by using a low flow rate in the ^{1}D, which is all directed to the ^{2}D. The low flow rate helps minimize solvent incompatibility with the ^{2}D solvent system and provides wider peaks to allow more fractions to be taken across the ^{1}D peaks, which minimizes undersampling and limits the sample amount on the ^{2}D column to facilitate peak refocusing. 2D-LC often uses very high flow rates in the ^{2}D to provide very fast runs so that several 2D runs can be accomplished over the width of a 1D peak to adequately reconstruct the peak profile. As Davis, Stoll, and Carr[9] discussed elsewhere, undersampling results when too few samples are taken across a peak.

Mondello and co-workers[10−12] have pioneered the use of comprehensive LC × LC for triacylglycerols (TAG) using Ag-ion chromatography, which does a partial separation into groups by degree of unsaturation coupled to nonaqueous reversed-phase (NARP) HPLC, which further separates into distinct peaks by partition number (PN), where the PN = # carbons − 2 × # double bonds. Their work included the use of atmospheric pressure chemical ionization (APCI) MS for detection. Others soon followed with solvent modifications, etc., aimed at providing improved separations,[13] and a variety of lipid applications.[14−18]

Received: July 14, 2017
Accepted: August 29, 2017
Published: August 29, 2017

DOI: 10.1021/acs.analchem.7b02753
Anal. Chem. 2017, 89, 10537−10546

One thing that most methods for TAG analysis by 2D-LC have in common is the use of silver-ion chromatography in the ^{1}D, followed by NARP UHPLC in the ^{2}D. This is due in large part to the commercial availability of silver-ion HPLC columns and the lack of availability of silver-ion UHPLC columns (and even a dearth of strong cation exchange (SCX) UHPLC columns from which to make silver-ion columns). Unfortunately, Ag-ion HPLC produces clusters of peaks, with TAGs having similar degrees of unsaturation appearing in only partially resolved clusters. This puts a greater demand on the ^{2}D NARP-UHPLC separation to resolve those clusters.

In contrast, we already had a NARP-HPLC separation[19] that we liked for 1D-LC and just wanted to use Ag-ion UHPLC to tease apart a few remaining overlaps and separate isomers. Therefore, we made our own silver-ion UHPLC column from one of the few SCX columns available, which we loaded with silver using an approach that differs from the classic approach that is still commonly used.[20] Our standard NARP-HPLC method[19] utilized a substantial amount of ACN, which caused a lack of retention on the silver-ion UHPLC column. Thus, we implemented a methanol/ethanol/dichloromethane (MeOH/EtOH/DCM) gradient for NARP-HPLC that is compatible with the Ag-ion second dimension. The resolution is not quite as good as our standard MeOH/ACN/DCM method, but this is compensated for by the separation in the ^{2}D.

Due to our earlier interest in the α-eleostearic acid (α-EA) (9*Z*,11*E*,13*E*-octadecatrienoic acid)-containing TAGs in the seed oil of cherry (*Prunus cerasus*) pit oil (CPO), the new approach was applied to the same CPO and to parinari (African Mobola Plum, *Parinari curatellifolia*) seed oil (PSO) and wild soybean (*Glycine soja*) oil (SBO). Primary emphasis is on PSO because, in addition to general nutrition parameters[21,22] (protein, fiber, moisture, ash, total fat), little more than the fatty acid (FA) composition has been previously reported,[21] with that being erroneous or incomplete, although some limited data for related species are also reported. There has been reference to α-EA in other parinari species,[23−25] which contributed to our interest in the samples reported here. We also extend our previous approach[19] beyond vitamin D analysis to other fat-soluble vitamins, specifically tocopherols in all three seed oils.

We report here the first demonstration of comprehensive 2D-LC with double dual parallel mass spectrometry. Two mass spectrometers operated in APCI-MS and ESI-high resolution accurate mass (HRAM)-MS modes as well as UV, a fluorescence detector (FLD), corona charged aerosol detector (CAD), and an evaporative light scattering detector (ELSD) were used to monitor the first dimension, coupled with two other mass spectrometers operated in atmospheric pressure photoionization (APPI)-MS and ESI-MS modes plus UV, for a comprehensive LC2MS4 (or LC1MS2 × LC1MS2) analysis. This approach allowed the first report of the diacylglycerol (DAG) and TAG composition of PSO, identification of a previously unreported oxo-FA, and the first report and quantification of tocopherols in PSO and improved analysis of tocopherols in CPO. Results were supplemented and confirmed by gas chromatography (GC) with a flame ionization detector (FID) and GC-MS in electron impact (EI) and chemical ionization (CI) modes.

EXPERIMENTAL SECTION

Due to the number of instruments used for LC2MS4, most instrument details are provided in the Supporting Information.

Column Preparation. An Epic-SCX strong cation exchange (SCX) column, 100 × 2.1 mm, 3 μm particles (#122191-ESCX), was obtained from ES Industries, Inc. An old Constametric 4100 MS quaternary HPLC pump was used to flush the SCX column with Millipore D.I. H_2O for at least an hour at 0.2 mL/min. Then, a 500 mL bottle of 1.0 M $AgNO_3$ solution (Sigma-Aldrich) was fitted with a cap and line and fed directly into the Y-fitting supplying the reciprocating pump heads. Initially, the outlet of the column was sent to waste; then, after ∼30 min, the outlet was directed back into the $AgNO_3$ bottle. The system was located in a room with subdued light, and the bottle of $AgNO_3$ was placed inside two closed nested boxes to eliminate light exposure. The solution was allowed to recycle through the column overnight at 0.2 mL/min, which represented ∼450 column volumes over 13 h. Next, the $AgNO_3$ was removed, and the column was flushed with D.I. H_2O at 0.2 mL/min for at least an hour. Finally, the column was flushed with MeOH at 0.2 mL/min for an hour, after which it was ready for use.

2D-LC Instrumentation. An Agilent 1200 HPLC system that employed two Inertsil ODS-2 columns in series, 250 × 4.6 mm, 5 μm particles, which has been described previously,[19] was used for the ^{1}D separation. A fluorescence detector (FLD) was added between the diode array detector (DAD) and flow splitter since the earlier report. A splitting system controlled flow to each detector based on the length and I.D. of the fused silica capillary directed to each instrument. Full details of all components are provided in the Supporting Information and are depicted in Figure 1. In summary, the ^{1}D was monitored

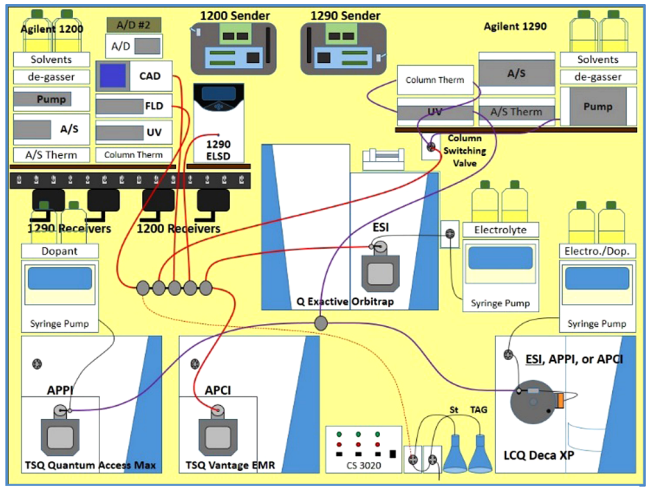

Figure 1. LC1MS4 configuration of instruments for comprehensive LC1MS2 × LC1MS2 plus UV, FLD, CAD, and ELSD.

using detection by a DAD, the FLD, the CAD, the ELSD (data not shown), a TSQ Vantage EMR mass spectrometer operated in APCI-MS mode, and a Q Exactive HRAM instrument operated in ESI-MS mode (with 20 mM NH_4OCOH in ACN, 1:4, at 20 μL/min via syringe pump). One branch of the splitter, having a flow rate of 53.67 μL/min, was directed to the Agilent G1170A switching valve with two 100 μL sample loops installed, producing a loop fill time of 1.86 min and modulation time of 1.91 min. The switching valve served as the interface to

DOI: 10.1021/acs.analchem.7b02753
Anal. Chem. 2017, 89, 10537−10546

an Agilent 1290 UHPLC system composed of a binary pump, column oven with the Epic-SCX/Ag-ion column installed, and DAD. Flow after the DAD no. 2 was directed to a single Valco tee splitter, with the two branches going to a TSQ Quantum Access Max mass spectrometer operated in APPI-MS mode with acetone dopant supplied by a dual piston syringe pump at 50 μL/min and an LCQ Deca XP ion trap mass spectrometer operated in ESI mode with 50 μL/min NH_4OCOH via syringe pump. Syringe pumps were AB140B/C dual piston syringe pumps. Syringe pumps for ESI instruments were plumbed through electronically controlled valves attached or built into the instruments to flush deionized water (from old HPLC pumps) through the sources between runs to reduce problems with clogging. Control of all instruments was coordinated using the 14-switch wireless communication contact closure system (WCCCS) previously described.[26] Visualization of the 2D-LC chromatograms was done using LC Image v. 2.5b7 software from GC Image, Inc.

GC Instrumentation. Analyses on an Agilent 6890N GC with a FID and an Agilent 7890A GC with 5975C MS (in EI and CI modes) were performed using the instruments and conditions recently reported.[27] Column and flow conditions are given in the Supporting Information.

Quantification. Calibration levels of 0.125, 0.250, 0.500, 1.00, and 2.00 μg/mL were prepared from 25.0 μg/mL (nominal) stock solutions of each fat-soluble vitamin (FSV) listed below with each concentration adjusted for standard purity (from Certificates of Analysis) and precise stock solution concentration. d_6-α-Tocopherol at 1.00 μg/mL was added as IS to all standards and samples. Quantification of FSVs by MS was done using APCI-MS in time-segmented selected ion monitoring (SIM) and selected reaction monitoring (SRM) modes using the parameters listed in the Supporting Information. Quantification of DAGs and TAGs was done using the GC-FID response-factor-adjusted approach previously described,[28,29] with inclusion of 1×^{13}C isotopic peaks for added sensitivity without loss of specificity, as previously discussed.[30] Quantification of FSVs by UV detection was done using wavelengths adapted from Ball,[31] specifically 297 nm for α-, γ-, and δ-tocopherols, 265 nm for vitamin D_2 and D_3, 326 nm for retinol (vitamin A), retinyl acetate, and retinyl palmitate, and 248 nm for phylloquinone (vitamin K_1). Fluorescence detection of tocopherols was done using a legacy detector (Agilent 1100 series) at 330 nm as a test of FLD specificity. Additional parameters for UV and FLD are given in the Supporting Information. All peaks were manually integrated, and calculations were performed using the linest() function in Excel spreadsheets using both IS and external standard approaches (ES).[19,30] Because the IS was optimized for MS detection, results by UV could only be estimated as discussed below.

RESULTS

We bypassed the problem of under-sampling and problems associated with quantification of 2D-LC "blobs" by directly monitoring the ^{1}D using two mass spectrometers, operated in APCI-MS and ESI-HRAM-MS modes as well as UV, FLD, CAD, and ELSD. Chromatograms and calibration lines of α-tocopherol by ^{1}D SIM and SRM are shown in Figure 2. Although we did not know to expect tocopherols in PSO, we routinely run samples using our FSV and TAG screening procedure, which allows quantification of any of the FSVs mentioned above if they are present. Table 1 shows the results

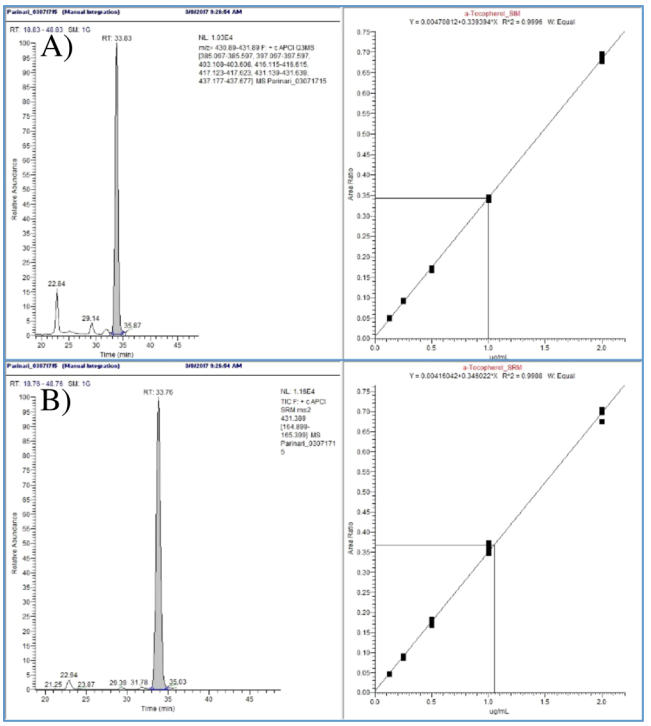

Figure 2. Chromatograms and calibration lines for α-tocopherol by (A) selected ion monitoring and (B) selected reaction monitoring. FA abbreviations: P, palmitic acid, 16:0 (carbons:double bonds); El, α-eleostearic acid, 9*c*,11*t*,13*t*-18:3 (*c* = cis, *t* = trans); L, linoleic acid, 18:2; O, oleic acid, 18:1; S, stearic acid, 18:0; G, gadoleic acid, 20:1; A, arachidic acid, 20:0.

Table 1. Quantification of α-, γ-, and δ-Tocopherols by SIM and SRM APCI-MS in ppm (μg/g Oil)

Selected ion monitoring, internal standard method						
	α	SD	γ	SD	δ	SD
cherry	293.5	3.5	630	26	97	14
parinari	789	28	881	45	6	16
soybean	29.9	0.3	168	14	227	13
r^2	0.9996		0.9883		0.9917	
Selected reaction monitoring, internal standard method						
	α	SD	γ	SD	δ	SD
cherry	281	12	897.8	5.4	120.8	6.9
parinari	806.3	1.3	1101	22	34.0	6.3
soybean	18.9	0.2	193.0	1.4	198	13
r^2	0.9988		0.9943		0.9956	

for the IS approach by SIM and SRM APCI-MS in ppm or μg/g of oil = mg/kg of oil with the first nonsignificant figure shown or to 0.1. The coefficients of determination (r^2) given in Table 1 indicate good linearity of the calibration lines. Results by the ES approach by APCI-MS and the IS and ES approaches by UV detection are given in the Supporting Information because these are all less desirable and reliable than the IS approach by MS. All ES and IS results by MS and UV, with the exception of UV results for α-tocopherol in PSO, were in good to excellent agreement among all approaches. To derive an estimation of IS results by UV required approximation of the IS integrated areas for 1.00 μg/mL as follows: the area for each α-tocopherol calibration standard was divided by the α-tocopherol total amount to give (area/(μg/mL)). Each area for all other FSVs was divided by the same-run normalized IS area. For samples,

DOI: 10.1021/acs.analchem.7b02753
Anal. Chem. 2017, 89, 10537−10546

the average normalized signal area across all standards (= 5.5294 ± 0.6330) was used as the IS area because it was unknown how much of the α-tocopherol was attributable to the IS and how much came from the oil sample. Again, no such approximation was required for results by ES or IS by MS or ES by UV.

FAs, DAGs, and TAGs. The FA composition calculated from the sum of response-factor-normalized DAGs and TAGs and by GC-FID for FAs present at ≥0.1% for *P. curatellifolia* is given in Table 2. Due to space limitations, all 18:3 species are grouped together in Table 2, as are all oxo-18:3 FA. A more detailed composition is provided in the Supporting Information. As identified by GC-MS and quantified by GC-FID, 90.0 ± 0.1% of 18:3 was α-eleostearic acid, 7.6 ± 0.1% was β-El, a third isomer (unidentified) represented 1.7 ± 0.0%, and only 0.1 ± 0.0% was normal Ln, and these comprise almost all of the 48.8% in Table 2. While eleostearic acid has been reported previously, this represents the first report of oxo-eleostearic acid in *P. curatellifolia*. Four oxo-El isomers were found by GC-MS and quantified by GC-FID, with the two major isomers representing 81.0 ± 0.8% and 13.3 ± 0.3%, comprising the majority of the 1.5% of oxo-El shown in Table 2. The compositions of DAGs and TAGs are given for the first time in Tables 3 and 4, respectively. DAGs represented only 1.52% of the total area of DAGs and TAGs. Figure 3 shows an ESI-HRAM-MS chromatogram and mass spectra of eleostearic acid and two oxygen functional group containing TAGs, and Figure 4 shows the APCI-MS data acquired in parallel. The $[M+NH_4]^+$ and $[M+H]^+$ ions for several TAGs had unexpected masses that were 14 mass units higher than those of normal eleostearic acid containing TAGs, with accompanying $[DAG]^+$ fragments at *m/z* 609.450 ($[ElEl+14]^+$). This mass difference could represent either a branched methyl-containing FA (−H + CH_3 = 14.0157) or an oxo-FA (−2H + O = 13.9793). Direct detection by HRAM ESI-MS in the ^{1}D allowed unambiguous differentiation of these two possibilities. The mass accuracy for normal, known TAGs were in the 2−4 ppm range, while for the possible methylated TAGs, the mass differences were 42−45 ppm for the $[M+NH_4]^+$ peaks and 62−63 ppm for the *m/z* 609.450 $[DAG]^+$ fragment. On the other hand, the calculated accurate masses for the oxo-eleostearic TAGs were within the 2−4 ppm range for all $[M+NH_4]^+$ and $[DAG]^+$ fragments (normal and ox-El), providing very strong evidence that the unknown TAG molecular species contained oxo-eleostearic acid. GC-MS chromatograms (not shown) exhibited a corresponding peak at *m/z* 306.2 representing the oxo-18:3 FAME. Finally, the chromatographic behavior of oxo-TAGs, which eluted prior to normal TAGs on the RP-HPLC column due to increased polarity, is consistent with expected behavior under RP-HPLC conditions. Several steps were taken to confirm that the oxo-TAGs were endogenous native species and were not formed during extraction. All data confirm the identification of multiple DAG and TAG molecular species containing oxo-eleostearic acid, shown in Tables 3 and 4, with oxo-TAGs being 4.65% of the response-factor-normalized TAG integrated area. The exact type and location of the oxo-

Table 2. FA Composition Calculated from DAG and TAG Composition of *P. cuatellifolia* Compared to FA from GC-FID of FA Methyl Esters

FA	average (%)	SD (%)	GC-FID (%)
P	9.1	0.0	9.3
El	48.8	0.1	48.8
L	14.4	0.1	14.0
O	17.7	0.1	17.5
S	7.3	0.1	7.6
A	0.4	0.0	0.4
G	0.7	0.0	0.7
oxo-El	1.6	0.0	1.5
sum	99.9		99.9

Table 3. Response Factor Normalized DAG Composition for *P. curatellifolia*

DAG	RT (1)[a]	% comp	DAG pk. 2/1[b]
oxElEl	19.09	0.7	0.21
oxElL	21.09	0.1	0.28
oxElO	26.30	0.2	0.23
oxElP	26.59	0.1	0.30
ElEl	32.46	17.4	2.57
PoO	35.68	0.8	1.61
LEl	35.84	11.2	2.72
LL	37.60	11.7	4.19
OEl	39.02	12.5	1.57
OL	39.77	14.7	3.43
PL	39.96	6.8	1.53
OO	41.73	6.9	1.50
OP	42.00	7.0	0.72
SL	42.55	4.8	1.59
OS	44.99	5.1	0.52
sum	99.9%		

[a]Retention time for first peak of the pair. [b]Ratio of DAG peak 2 to DAG peak 1.

Table 4. Response Factor Normalized TAG Composition for *P. curatellifolia*

TAG	RT	% comp	TAG	RT	% comp
oxElElEl	46.02	1.3	POL	75.30	2.1
oxElElL	47.08	0.4	LLS	76.15	0.5
oxElElO	50.54	0.9	PPL	77.15	0.7
oxElElP	51.23	0.7	LElA	79.48	0.3
oxElLO	51.87	0.1	ElElA	79.89	0.5
oxElOO	56.21	0.1	SOEl	82.19	3.0
oxElElS	56.26	0.9	OOO	82.21	1.0
oxElOP	56.83	0.1	OLG	82.29	0.3
oxElOS	63.36	0.1	OOP	84.24	1.4
ElElEl	55.11	12.0	ElSP	84.32	1.0
ElElL	56.70	8.3	PLG	84.37	0.2
LLEl	58.47	3.3	SLO	85.04	1.4
LLL	60.31	0.4	POP	86.29	0.5
ElElO	62.05	11.3	SLP	87.09	0.9
ElElP	63.23	8.1	OOG	90.98	0.1
OLEl	64.10	7.8	ElOA	91.46	0.1
PLEl	65.44	4.6	OOS	93.68	0.8
LLO	66.33	1.0	ElSS	93.83	0.9
LLP	67.64	0.9	POS	95.79	0.7
ElElG	68.65	1.3	PLA	96.36	0.1
ElElS	70.83	8.9	SSL	96.38	0.4
OOEl	70.94	4.2	PPS	99.31	0.1
POEl	72.50	3.0	POA	104.09	0.1
LLG	73.27	0.2	SSO	104.19	0.3
OOL	73.53	1.8	sum		99.3
PPEl	74.35	0.4	oxo-TAG		4.65

DOI: 10.1021/acs.analchem.7b02753
Anal. Chem. 2017, 89, 10537−10546

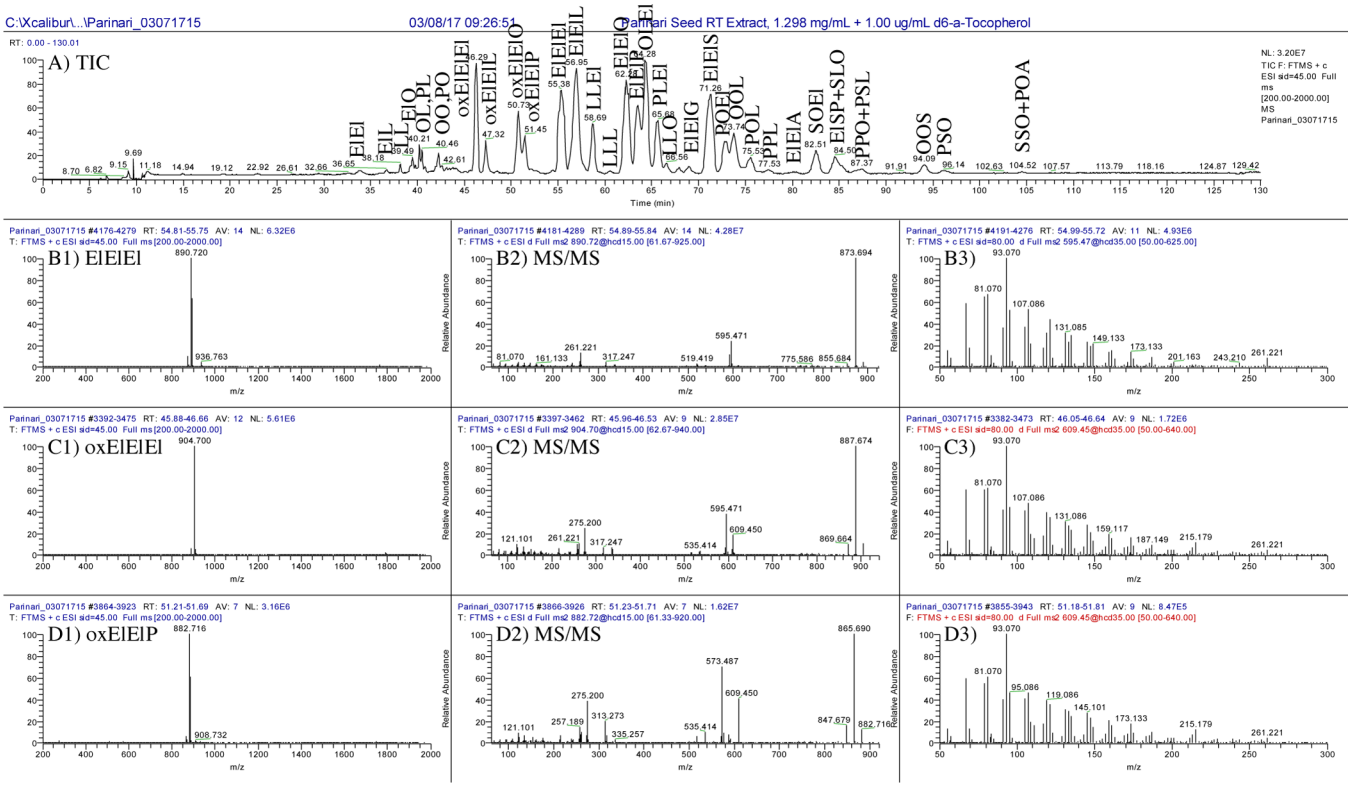

Figure 3. Q Exactive Orbitrap ESI-HRAM-MS total ion current chromatogram (TIC) and mass spectra for trieleostearin, ElElEl, and two TAGs containing previously unidentified oxo-eleostearic acid, oxElElEl, and oxElElP (column 1); low-energy CID MS/MS of $[M+NH_4]^+$ (column 2); and higher-energy CID of m/z 595 or m/z 609 $[DAG]^+$ fragment (column 3). FA abbreviations are in the Experimental Section.

functional group could not be determined from the mass spectra alone. However, comparison of the MS/MS spectra from ElElEl and oxElElEl in Figure 3 hint that the oxo-group is not at the distal end of the FA chain, and differences in the m/z 105−111 (= C_8H_x) and m/z 117−119 (= C_9H_x) peaks indicate the possibility that it is an 8,9-oxo group. Unfortunately, time, resources, and stakeholder interest will not allow us to pursue identification of the exact identity of this oxo-FA. The early eluting peaks should be collected and subjected to IR and NMR analysis. We will be happy to share all LC-MS data. Finally, there was both HRAM ESI-MS ($[M+NH_4]^+$= m/z 918.681 observed) and APCI-MS ($[M + H]^+$= m/z 901.6 obs) evidence for the dioxo TAG oxEloxElEl present at a very low level at earlier retention time, which was not quantified.

The FA, DAG, and TAG compositions for cherry pit and wild SBO are given in the Supporting Information because these have been reported previously and were used for verification of the new approach. All results for CPO are in good agreement with the results reported recently using 1D NARP-HPLC.[27] The SBO FA, DAG, and TAG compositions are similar to results reported elsewhere, although previous reports focused primarily on *Glycine max* commercially produced soybeans rather than the wild type.

Second-Dimension (^{2}D) Data. A contour plot for *P. curatellifolia* by silver-ion UHPLC with APPI-MS detection is shown in Figure 5 and that by ESI-MS is shown in Figure 6. Corresponding 3D plots are given in Figures 7 and 8. As usual, ESI-MS exhibits sensitivity greater than that of either APCI-MS or APPI-MS, giving larger peaks in Figures 6 and 8. No attempt was made to quantify the DAGs and TAGs using the contour plots because these are known to be problematic for quantification,[6,32−35] and very effective quantification using a well-established approach was provided by the ^{1}D APCI-MS data. The ^{2}D data were used only for qualitative analysis. The silver-ion UHPLC column provided a separation based on the well-known principles that have been described for argentation chromatography in the past. Boryana Nikolova-Damyanova and William W. Christie provide an excellent tutorial for argentation chromatography at the Lipid Library (http://lipidlibrary.aocs.org/content.cfm?ItemNumber=40341). Because *cis* double bonds produce stronger complexes with silver ions than *trans* double bonds,[36] the UHPLC column described here very effectively separated ElElEl containing all α-eleostearic acid from ElElEl containing a β-eleostearic acid FA, as seen in Figures 5 and 6. Thus, comprehensive NARP-HPLC × Ag-ion-UHPLC appears to be well-suited for differentiating *cis*/*trans* isomers in TAGs.

Also, the position of the unsaturated FAs in TAGs has a primary influence on the retention on the Ag-ion UHPLC column, with those in the outer positions, i.e. 1 and 3, having a stronger effect on retention than those in the middle, *sn*-2, position. For example, Figure 9 shows a ^{2}D UHPLC ESI-MS EIC for m/z 904.8, which represents multiple isobaric TAG molecular species and their isomers.

First, this shows that most peaks eluted in single, unsplit peaks, although some (e.g., OSO) straddled two modulation periods separated by the modulation time, as shown for OSO in Figure 9. This greatly simplified interpretation of data and gave the sharp peaks exemplified in Figures 7 and 8. Second, the silver-ion column readily differentiated between two oleic acid chains in the 1,2 positions in OOS from two oleic chains in the 1,3 positions in OSO. However, because retention was based on degree of unsaturation, with minimal effect of chain length, OSO and GPO, which both have two monounsaturated FAs in

DOI: 10.1021/acs.analchem.7b02753
Anal. Chem. 2017, 89, 10537−10546

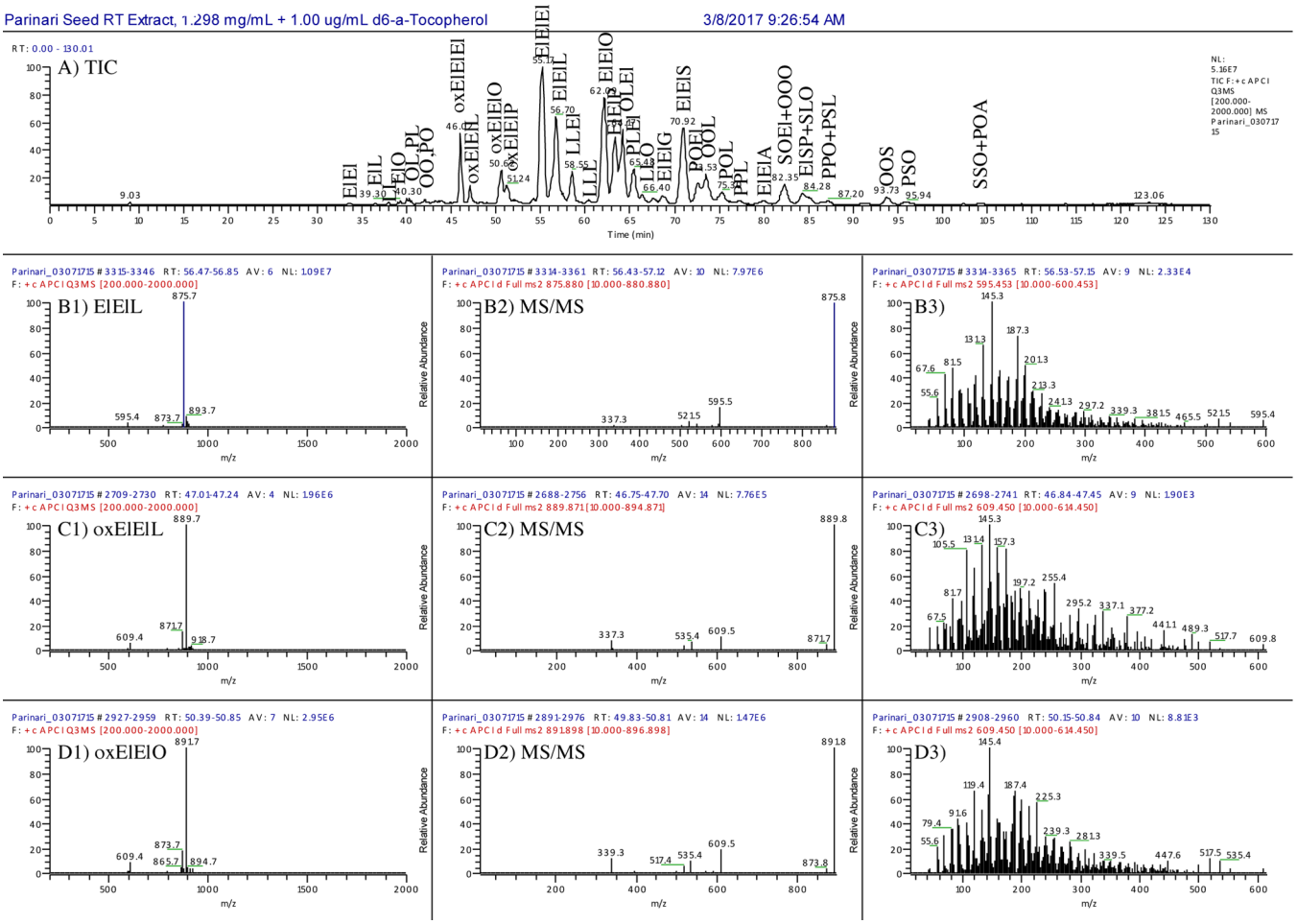

Figure 4. TSQ Vantage EMR APCI-MS TIC and mass spectra for ElElL, oxElElL, and oxElElO (column 1), low-energy CID MS/MS of $[M + H]^+$ (column 2), and higher-energy CID of m/z 595 or m/z 609 $[DAG]^+$ fragment (column 3). FA abbreviations are in the Experimental Section. See Table 4 for TAG composition from APCI-MS.

the 1,3 positions were not separated, although these could be distinguished by the different $[DAG]^+$ fragments despite having one $[DAG]^+$ fragment, m/z 605.5, and the protonated molecule mass in common. Similarly, SLS was differentiated from SSL due to the different position of the "L" FA. But SLS was not separated from PLA, which has different saturated FA chain lengths at 1 and 3, but the "L" FA in the same *sn*-2 position. In general, the first row of TAGs eluted in Figures 5 and 6 had one or no *cis* double bonds in one of the 1 or 3 positions with one or no *cis* double bonds in the *sn*-2 position, with the exception of oxo-El, in which the oxo- group appeared to reduce coordination of El with the Ag^+ and reduce retention (i.e., oxElElEl). The second row of TAGs had either two *cis* double bonds in the 1 or 3 positions or one diunsaturated FA (i.e., "L") in the *sn*-2 position. Additional unsaturation in the 1,3 positions had a greater influence on retention with additional unsaturation in the *sn*-2 position having a slightly lesser effect on retention, as mentioned above. Because APPI-MS and ESI-MS were used for detection in the ^{2}D, assignment of regioisomer identities by the Critical Ratio[37,38] $[AA]^+/[AB]^+$ by MS was less reliable[38] than by APCI-MS. For instance, the difference in $[OO]^+/[OS]^+$ between OOS sand OSO(2) in Figure 9 is not as large as expected or reported using APCI-MS.[39] Fortunately, Ag-ion UHPLC was very effective for separating regioisomers, reducing the need to rely on fragment ratios in ESI-MS/MS or APPI-MS mass spectra.

DISCUSSION

Although complete details are not given, Powell[40] described producing a silver-ion column from a sulfonate derivatized silica column by flowing silver nitrate through the column. Although we were not initially aware of that work, we used a similar approach, differing primarily in the fact that we employed exhaustive saturation by recycling $AgNO_3$ through a commercially available SCX column overnight. Both approaches contrast the more commonly used approach by Christie[20] of manually injecting $AgNO_3$ solution, which has been widely used to good effect. In the first sequence of runs immediately after preparation of a new column, small amounts of silver adducts were formed during ESI-MS, but these quickly disappeared with further use. No corrosive effects of $AgNO_3$ elution were observed in the ionization source of any instrument. This approach has been used both for 1.8 μm particle and 3.0 μm particle columns, but we prefer the latter for increased robustness.

It is important to emphasize that the excellent quantitative results reported here would not be possible using conventional comprehensive 2D-LC approaches. Quantification of ^{2}D 2D-LC data is an ongoing area of development,[32] but is not yet as straightforward as conventional integration of 1D or ^{1}D chromatograms. As mentioned by Place et al.,[33] each 2D peak consists of individual 1D chromatograms (slices) that

DOI: 10.1021/acs.analchem.7b02753
Anal. Chem. 2017, 89, 10537−10546

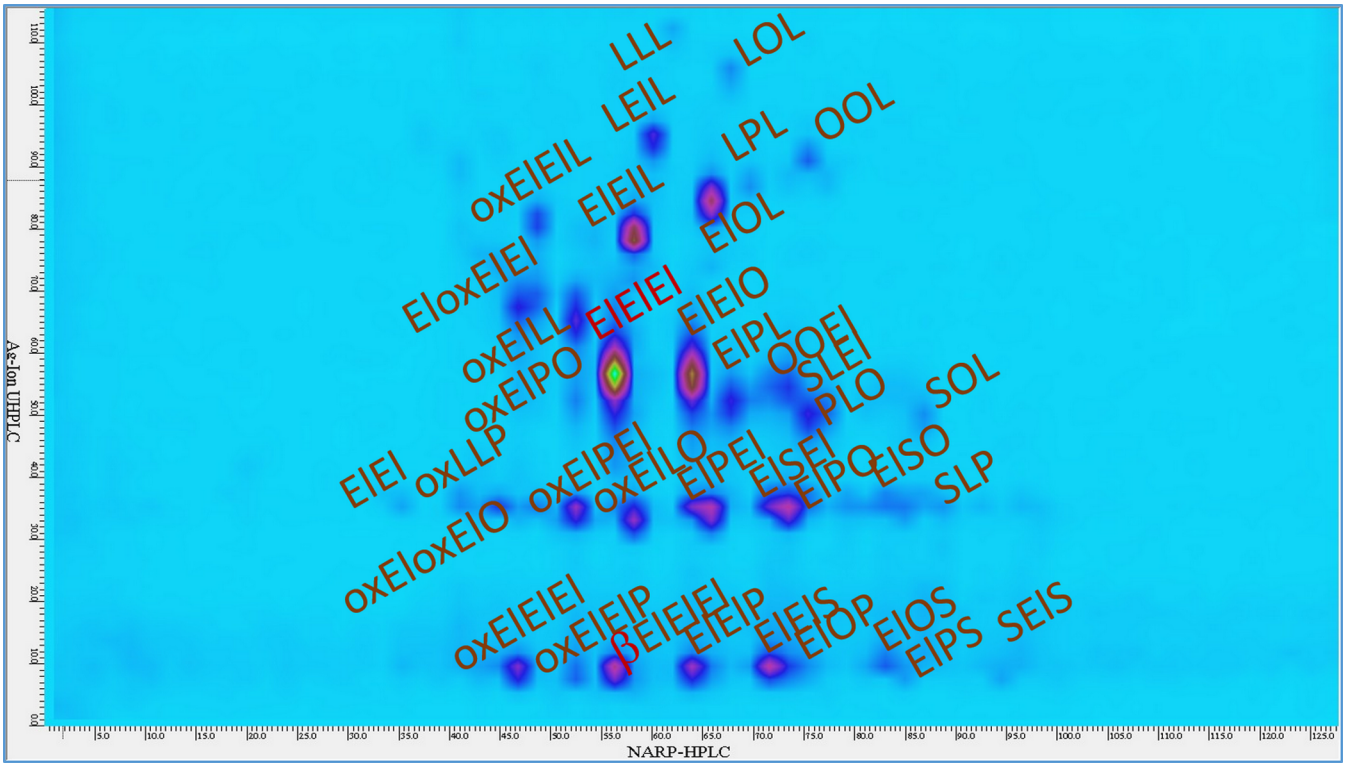

Figure 5. Second dimension silver-ion UHPLC separation with APPI-MS of *P. curatellifolia* seed oil.

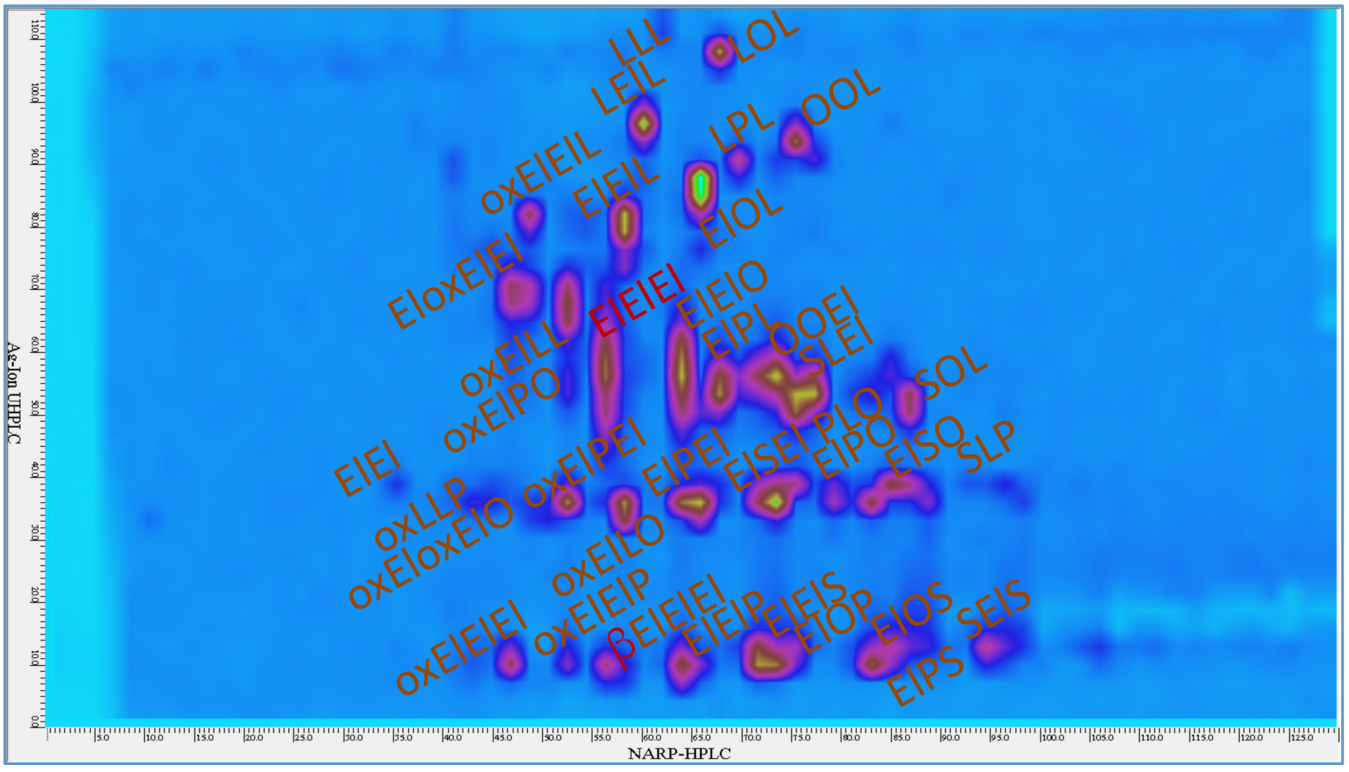

Figure 6. Second dimension silver-ion UHPLC separation with ESI-MS of *P. curatellifolia* seed oil.

would normally be manually integrated in 1D analysis. But having numerous slices across each 2D peak makes such integration impractical. So, they described several approaches for automated integration of 2D peaks, which involved lab-written procedures in the R programming language. Cook et al.[34] discussed the several-fold higher %RSDs encountered in 2D-LC and the reasons for these and many other factors, including the poorer S/N due to peak dilution caused by peak fractionation. They employed a single UV detector at the outlet of the ^{1}D, for 2D assisted LC, or 2DALC. Recently, targeted

DOI: 10.1021/acs.analchem.7b02753
Anal. Chem. 2017, 89, 10537−10546

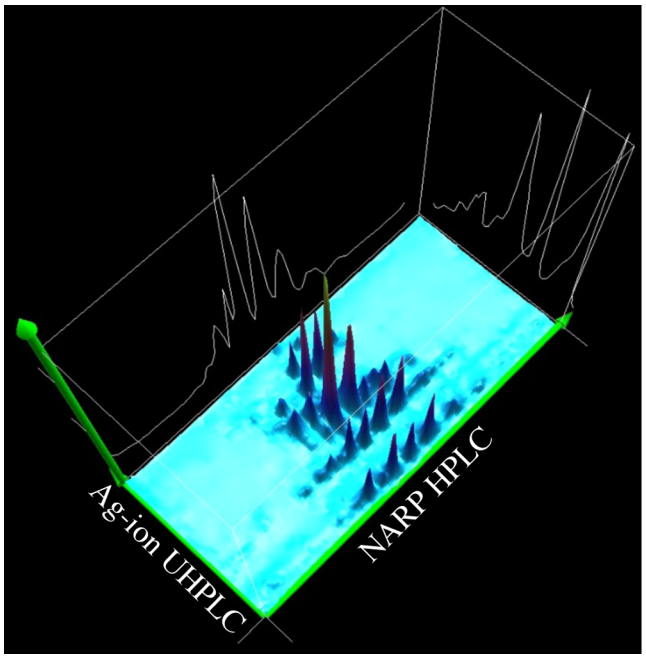

Figure 7. 3D plot of Ag-ion UHPLC APPI-MS for *P. curatellifolia*.

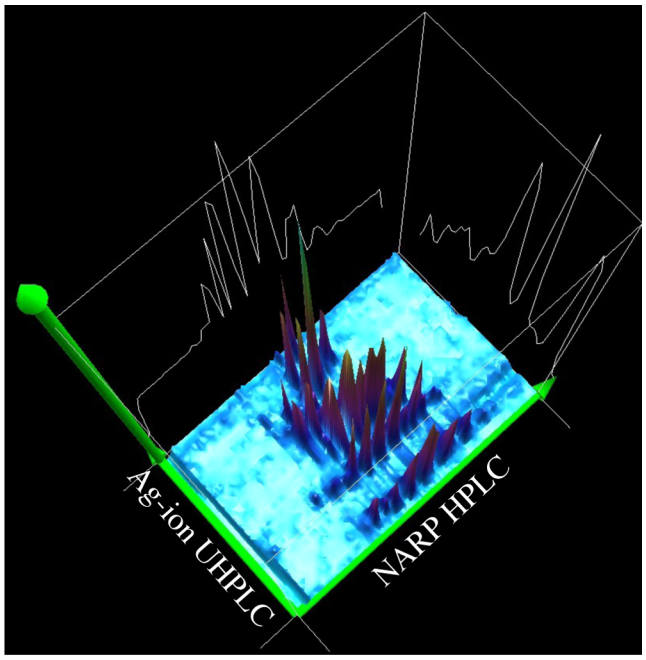

Figure 8. 3D plot of Ag-ion UHPLC ESI-MS for *P. curatellifolia*.

quantitative MS analysis of two target compounds using multiple reaction monitoring (MRM) was combined with qualitative analysis of wine polyphenols.[35] But because we wanted to quantify multiple FSVs and semiquantify a large number of DAGs and TAGs (by relative percentage composition), we took an approach similar to 2DALC but with many more detectors.

Quantification of CPO tocopherols was included because the extract-and-shoot approach gave values that were substantially higher than those values reported by a commercial lab in our recent report. The results reported earlier were obtained using the traditional approach to sterol analysis, involving heated saponification, extraction, and collection of unsaponifiable material and derivatization followed by GC-FID analysis. By eliminating all harsh and inefficient treatment such as saponification and derivatization, we observed higher levels. Additional work is underway to confirm these results by analysis of standard reference material 3278 from the National Institute of Standards and Technology. Furthermore, the use of both SIM and SRM (often thought of as the "gold standard" for analysis) MS provided very strong confirmation of tocopherol identity as well as quantity. Additionally, by obtaining survey MS and data-dependent MS/MS scans on all instruments, we are able to refute the presence of β-sitosterol that was reported by the same commercial lab using the same saponification, extraction and collection, and derivatization approach in CPO. Using APCI-MS EICs for a 5 Da mass range including γ-tocopherol (Table 1) ($[M + H]^+ = m/z$ 417.4) and β-sitosterol ($[M + H]^+ = m/z$ 415.4), we were able to clearly see the peaks for γ-tocopherol but not β-sitosterol. This demonstrates that peaks at a given retention time by GC without confirmation by MS, especially after extensive chemical pretreatment, are not sufficient for identification and quantification. Thus, it is advisible to view commercial lab results that do not include MS with healthy skepticism. Similar skepticism should be applied to SIM versus SRM results. Any interfering species that produce fragments or other ions similar to target compounds can skew SIM results. SRM is a more selective process, providing a higher degree of confidence. Nevertheless, because this approach has not yet been validated using a standard reference material (underway), these results for tocopherols are preliminary results.

Skepticism was also applied to observation of the oxo-FA, oxo-DAGs, and oxo-TAGs. To prove that these were not produced by oxidation during the Folch extraction process, we conducted experiments in which all solvents were deaerated with argon, and extractions were done using both cold solvents and room temperature solvents. The oxo-DAGs and oxo-TAGs were present in all samples regardless of treatment. Thus, we can conclude that these did contain uncommon oxo-FAs. We doubt that these are hydroxyl-FAs because they lack the very common dehydration products, $-H_2O = \Delta 18$ Da, that appear with large abundances in ESI-MS/MS and APCI-MS spectra of hydroxyl-TAGs.[41,42]

It should be pointed out that the ^{2}D solvent system (MeOH/ACN) is entirely compatible and miscible with the ^{1}D solvent system (MeOH/EtOH/DCM), thereby eliminating all compatibility issues that can arise using hexane-based solvent systems for Ag-ion HPLC. Also, the column-switching valve was plumbed in countercurrent mode (first in, last out) because the polyunsaturated TAGs that eluted first in the ^{1}D eluted last in the ^{2}D. Furthermore, *cis*-polyunsaturated DAGs and TAGs did not elute from the Ag-ion UHPLC column until the ACN content reached a sufficient level, so there was a degree of sample reconcentration at the head of the column, contributing to the sharp peaks seen in Figures 7 and 8.

When referring to the 1 and 3 positions of the glycerol backbone, we no longer use the designation *sn* (stereospecific numbering), because NARP HPLC, Ag-ion UHPLC, ESI-MS, APCI-MS, and APPI-MS are not capable of distinguishing enantiomers. The only position that can be known from these data is the *sn*-2 position. Chiral chromatography is required to differentiate the *sn*-1 and *sn*-3 positions. Therefore, the labels for the 1 and 3 positions are interchangeable unless chiral chromatography has been applied.

DOI: 10.1021/acs.analchem.7b02753
Anal. Chem. 2017, 89, 10537−10546

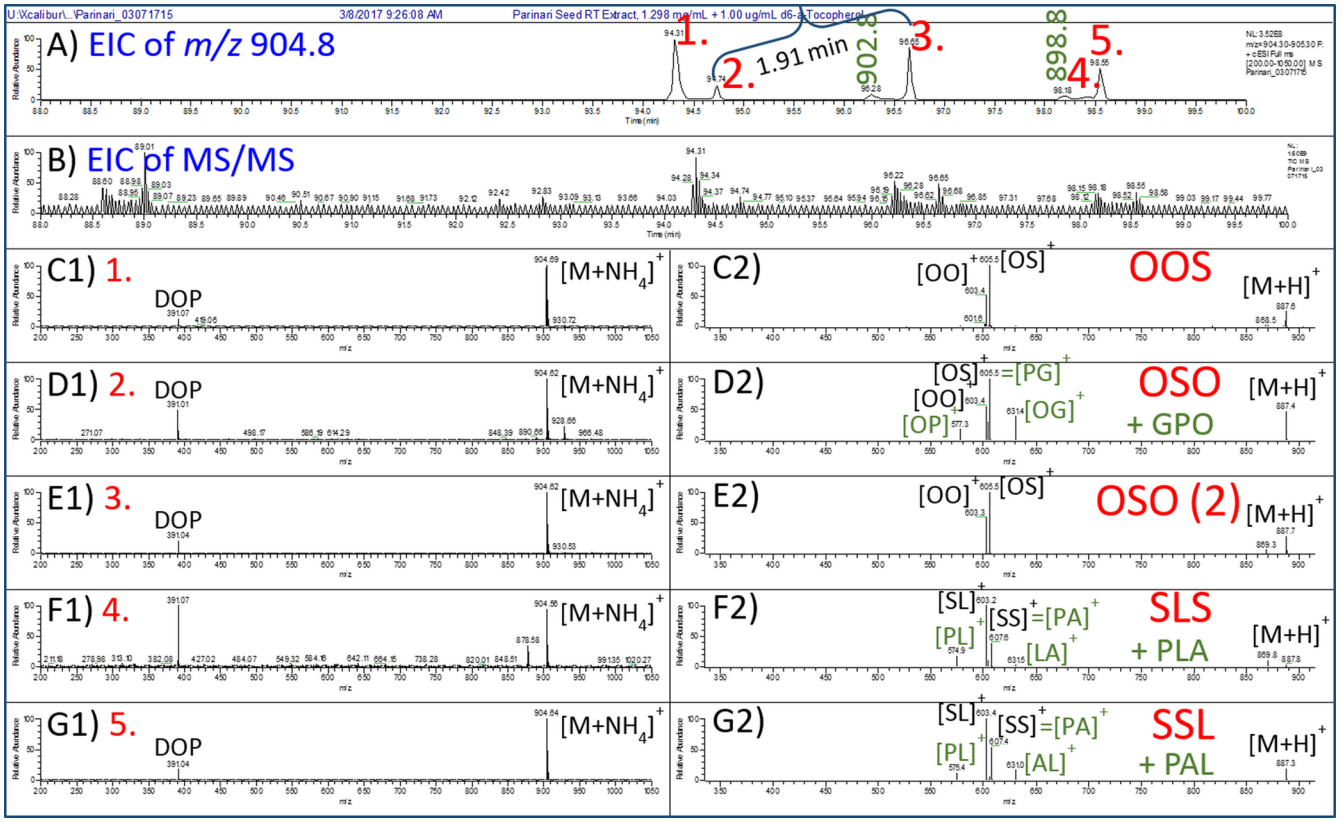

Figure 9. Extracted ion chromatograms and mass spectra of *m*/*z* 904.8 by Ag-ion UHPLC ESI-MS and MS/MS showing differentiation of regioisomers. DOP: dioctyl phthalate (plasticizer). FA abbreviations are in the Experimental Section.

An interesting observation that was unique to PSO was the difference in the ratios of the intact DAG peaks shown in Table 3 (in the column labeled DAG pk. 2/1). In most seed oils, the 1,2 + 2,3-DAG peak elutes earlier and is ∼2 times larger than the 1,3-DAG peak, which is smaller and elutes just after the larger peak. In PSO, even normal DAGs like LL showed a larger second peak as well as El-containing DAGs like ElEl and EllL and oxo-DAGs, oxo-ElEl, oxo-EllL, etc.

Another interesting observation was that APCI-MS and MS/MS spectra of di-El containing TAGs (ElElEl, ElElL, ElElO, etc.) showed almost exclusively the $[ElEl]^+$ $[DAG]^+$, *m*/*z* 595.5, with very little of the $[ElX]^+$ $[DAG]^+$ fragment. This unique behavior may indicate the possibility of cross-linking of the di-El FA chains during ionization in the APCI source, making it energetically unfavorable for formation of the $[ElX]^+$ fragment. This possibility was also indicated by the appearance of more of a *m*/*z* 593 fragment in ESI-MS/MS and APCI-MS mass spectra (Figures 4 and 5) than is formed from normal LnLnLn, which forms virtually only the expected *m*/*z* 595.5. Furthermore, TAGs containing oxElEl behaved in a similar manner, producing *m*/*z* 609.5 with little or no $[EllL]^+$, $[ElO]^+$, or other related $[DAG]^+$ fragments, as in Figure 4.

Finally, some readers may believe that this system of two chromatographs with four mass spectrometers is prohibitively complex or expensive and cannot readily be replicated. We want to point out that researchers may take aspects of the experiments that are needed and leave unnecessary parts behind. If we had only one mass spectrometer for the ^{1}D, we would use the HRAM Q Exactive Orbitrap instrument in APCI-MS mode. This would still allow identification of unknowns by HRAM MS, while also allowing quantification of FSVs, most of which do not respond well to ESI-MS without derivatization. Some may not be interested in 2D-LC at all, but the demonstration of Ag-ion UHPLC can be applied to standalone UHPLC in new ways. This arrangement of experiments was not expensive, because the slow ^{2}D chromatography and maintaining and repairing instruments ourselves allows us to keep older, inexpensive instruments in service, providing valuable data long after they have been retired elsewhere. The WCCCS system was not at all expensive, makes switching between instruments in experiments very easy, and would be a valuable addition to any LC-MS lab. Thus, while we demonstrated an unprecedented series of experiments that employ a novel arrangement of instruments, many of the components and concepts can be taken and applied individually to address a wide variety of analytical problems.

CONCLUSIONS

This work represents the first report of an application employing comprehensive 2D-LC with quadruple parallel mass spectrometry, or LC1MS2 × LC1MS2, for an LC2MS4 approach. Also reported here are the first examples of production of a silver-ion UHPLC column for triacylglycerol analysis, Ag-ion UHPLC, and Ag-ion UHPLC used as the ^{2}D in comprehensive 2D-LC. This work provides the first description of intact DAGs and TAGs from *P. curatellifolia* seed oil, of an oxo-FA in *P. curatellifolia* along with its confirmation using HRAM ESI-MS and GC-MS, and the first quantification of oxo-DAGs and oxo-TAGs for PSO. APCI-MS data provided indications of unique ionization and fragmentation mechanisms occurring in the APCI source for TAGs containing conjugated *trans* double bonds. This work provides the first quantification

DOI: 10.1021/acs.analchem.7b02753
Anal. Chem. 2017, 89, 10537−10546

of tocopherols in *P. curatellifolia* and shows the benefit of an extract-and-shoot approach for tocopherols in cherry pit oil. Further, these experiments describe the use of slow comprehensive 2D-LC, in which the problem of undersampling is bypassed by direct detection using six detectors in the ^{1}D. This allowed more flexibility in ^{2}D method development and instruments to be used that were older than those in conventional fast 2D-LC. The Ag-ion UHPLC column was ideal for separation of TAGs by type of double bond (*cis* versus *trans*) and of regioisomers based on the locations of unsaturated FAs, either in the 1,3 positions or the *sn*-2 position. These experiments employed a unique wireless communication contact closure system to coordinate all instruments.

■ ASSOCIATED CONTENT

Supporting Information

The Supporting Information is available free of charge on the ACS Publications website at DOI: 10.1021/acs.analchem.7b02753.

Experimental details for the Folch extraction, FAME preparation, GC-FID, and GC-MS analysis conditions, HPLC and UHPLC systems, and all mass spectrometers; external standard results for tocopherols by APCI-MS and internal standard and external standard results by UV detection; detailed compositions of FAMEs, DAGs, and TAGs for PSO, CPO, and SBO; and ^{2}D UHPLC contour plots for CPO and SBO (PDF)

■ AUTHOR INFORMATION

Corresponding Author

*E-mail: C.Byrdwell@ars.usda.gov.

ORCID

William C. Byrdwell: 0000-0001-8241-428X

Notes

The author declares no competing financial interest.

■ ACKNOWLEDGMENTS

The work of Dr. Robert Goldschmidt to extract the oil and perform the analysis of fatty acid methyl esters by GC-FID and confirmation of identities by GC-MS is gratefully acknowledged. The work of Mr. Lucas Stolp and Dr. Dharma Kodali to provide the CPO sample is gratefully acknowledged. This work was supported by the USDA Agricultural Research Service. Mention or use of specific products or brands does not represent or imply endorsement by the USDA.

■ REFERENCES

(1) Dugo, P.; Cacciola, F.; Kumm, T.; Dugo, G.; Mondello, L. *J. Chromatogr. A* **2008**, *1184*, 353−368.
(2) Malerod, H.; Lundanes, E.; Greibrokk, T. *Anal. Methods* **2010**, *2*, 110−122.
(3) Bedani, F.; Schoenmakers, P. J.; Janssen, H. G. *J. Sep. Sci.* **2012**, *35*, 1697−1711.
(4) Donato, P.; Cacciola, F.; Tranchida, P. Q.; Dugo, P.; Mondello, L. *Mass Spectrom. Rev.* **2012**, *31*, 523−559.
(5) Cacciola, F.; Donato, P.; Mondello, L.; Dugo, P. In *Handbook of Advanced Chromatography/Mass Spectrometry Techniques*; Holčapek, M., Byrdwell, W. C., Eds.; Elsevier/AOCS Press: Champaign, IL, 2017; pp 350−450.
(6) Stoll, D. R. In *Handbook of Advanced Chromatography/Mass Spectrometry Techniques*; Holčapek, M., Byrdwell, W. C., Eds.; Elsevier/AOCS Press: Champaign, IL, 2017; pp 250−350.
(7) Marriott, P. J.; Schoenmakers, P.; Wu, Z. Y. *LC-GC Eur.* **2012**, *25*, 1.
(8) Schoenmakers, P.; Marriott, P.; Beens, J. *LC-GC Eur.* **2003**, *16*, 335−339.
(9) Davis, J. M.; Stoll, D. R.; Carr, P. W. *Anal. Chem.* **2008**, *80*, 461−473.
(10) Mondello, L.; Tranchida, P. Q.; Stanek, V.; Jandera, P.; Dugo, G.; Dugo, P. *J. Chromatogr. A* **2005**, *1086*, 91−98.
(11) Dugo, P.; Kumm, T.; Crupi, M. L.; Cotroneo, A.; Mondello, L. *J. Chromatogr. A* **2006**, *1112*, 269−275.
(12) Dugo, P.; Kumm, T.; Chiofalo, B.; Cotroneo, A.; Mondello, L. *J. Sep. Sci.* **2006**, *29*, 1146−1154.
(13) van der Klift, E. J. C.; Vivó-Truyols, G.; Claassen, F. W.; van Holthoon, F. L.; van Beek, T. A. *J. Chromatogr. A* **2008**, *1178*, 43−55.
(14) Yang, Q.; Shi, X.; Gu, Q.; Zhao, S.; Shan, Y.; Xu, G. *J. Chromatogr. B: Anal. Technol. Biomed. Life Sci.* **2012**, *895*−*896*, 48−55.
(15) Wei, F.; Ji, S. X.; Hu, N.; Lv, X.; Dong, X. Y.; Feng, Y. Q.; Chen, H. *J. Chromatogr. A* **2013**, *1312*, 69−79.
(16) Hu, J.; Wei, F.; Dong, X. Y.; Lv, X.; Jiang, M. L.; Li, G. M.; Chen, H. *J. Sep. Sci.* **2013**, *36*, 288−300.
(17) Bang, D. Y.; Moon, M. H. *J. Chromatogr. A* **2013**, *1310*, 82−90.
(18) Holčapek, M.; Ovčačíková, M.; Lísa, M.; Cífková, E.; Hájek, T. *Anal. Bioanal. Chem.* **2015**, *407*, 5033−5043.
(19) Byrdwell, W. C. *Anal. Bioanal. Chem.* **2011**, *401*, 3317−3334.
(20) Christie, W. W. *J. High Resolut. Chromatogr.* **1987**, *10*, 148−150.
(21) Ogungbenle, H. N.; A, A. A. *Br. Biotechnol. J.* **2014**, *4*, 379−386.
(22) Abolaji, O. A.; Adebayo, A. H.; Odesanmi, O. S. *Pak. J. Nutr.* **2007**, *6*, 665−668.
(23) Chisholm, M. J.; Hopkins, C. Y. *J. Am. Oil Chem. Soc.* **1966**, *43*, 390−392.
(24) Cornelius, J. A.; Hammonds, T. W.; Leicester, J. B.; Ndabahweji, J. K.; Rosie, D. A.; Shone, G. G. *J. Sci. Food Agric.* **1970**, *21*, 49−50.
(25) Sommerfeld, M. *Prog. Lipid Res.* **1983**, *22*, 221−233.
(26) Byrdwell, W. C. *J. Lab. Autom.* **2014**, *19*, 461−467.
(27) Korlesky, N. M.; Stolp, L. J.; Kodali, D. R.; Goldschmidt, R.; Byrdwell, W. C. *J. Am. Oil Chem. Soc.* **2016**, *93*, 1−11.
(28) Byrdwell, W. C.; Neff, W. E.; List, G. R. *J. Agric. Food Chem.* **2001**, *49*, 446−457.
(29) Byrdwell, W. C.; Emken, E. A.; Neff, W. E.; Adlof, R. O. *Lipids* **1996**, *31*, 919−935.
(30) Byrdwell, W. C. *J. Chromatogr. A* **2013**, *1320*, 48−65.
(31) Ball, G. F. M. *Fat-Soluble Vitamin Assays in Food Analysis: A Comprehensive Review*; Elsevier Science Publishing: New York, 1988.
(32) Matos, J. T. V.; Duarte, R. M. B. O.; Duarte, A. C. *J. Chromatogr. B: Anal. Technol. Biomed. Life Sci.* **2012**, *910*, 31−45.
(33) Place, B. J.; Morris, M. J.; Phillips, M. M.; Sander, L. C.; Rimmer, C. A. *J. Chromatogr. A* **2014**, *1368*, 107−115.
(34) Cook, D. W.; Rutan, S. C.; Stoll, D. R.; Carr, P. W. *Anal. Chim. Acta* **2015**, *859*, 87−95.
(35) Donato, P.; Rigano, F.; Cacciola, F.; Schure, M.; Farnetti, S.; Russo, M.; Dugo, P.; Mondello, L. *J. Chromatogr. A* **2016**, *1458*, 54−62.
(36) Morris, L. J. *J. Lipid Res.* **1966**, *7*, 717−732.
(37) Byrdwell, W. C. *Anal. Bioanal. Chem.* **2015**, *407*, 5143−5160.
(38) Byrdwell, W. C. *J. Am. Oil Chem. Soc.* **2015**, *92*, 1533−1547.
(39) Fauconnot, L.; Hau, J.; Aeschlimann, J. M.; Fay, L. B.; Dionisi, F. *Rapid Commun. Mass Spectrom.* **2004**, *18*, 218−224.
(40) Powell, W. S. *Anal. Biochem.* **1981**, *115*, 267−277.
(41) Byrdwell, W. C.; Neff, W. E. *J. Liq. Chromatogr. Relat. Technol.* **1998**, *21*, 1485−1501.
(42) Byrdwell, W. C.; Neff, W. E. *Rapid Commun. Mass Spectrom.* **2002**, *16*, 300−319.

DOI: 10.1021/acs.analchem.7b02753
Anal. Chem. 2017, 89, 10537−10546